Effect of the microstructure of n-butyl acrylate/N-isopropylacrylamide copolymers on their thermo-responsiveness, self-organization and gel properties in water

Fang Yin, Juliette Behra, Mariana Beija, Annie Brûlet, Juliette Fitremann, Bruno Payre, Stéphane Gineste, Mathias Destarac, Nancy Lauth de Viguerie, Jean-Daniel Marty

Effect of the microstructure of *n*-butyl/*N*-isopropylacrylamide copolymers on their thermo-responsiveness, self-organization and gel properties in water

Fang Yin,[1] Juliette S. Behra,[1] Mariana Beija,[1] Annie Brûlet,[2] Juliette Fitremann,[1] Bruno Payré,[3] Stéphane Gineste,[1] Mathias Destarac,[1] Nancy Lauth-de Viguerie[1*] and Jean-Daniel Marty,[1*]

[1] IMRCP, UMR 5623, CNRS, Université de Toulouse, 118 route de Narbonne, F-31062 Toulouse, France

[2] Université Paris-Saclay, CNRS, CEA, Laboratoire Léon Brillouin, CEA Saclay, F-91191 GIF/Yvette, France.

[3] CMEAB, IFR-BMT, Université de Toulouse, 133 route de Narbonne, 31062 Toulouse, France

*corresponding authors. Tel. +33.56155.6135. E-mail: viguerie@chimie.ups-tlse.fr, marty@chimie.ups-tlse.fr

ABSTRACT.

Hypothesis: Polymer composition, microstructure, molar mass, architecture… critically affect the properties of thermoresponsive polymers in aqueous media.

Experiments: The behaviour of *n*-isopropylacrylamide and *n*-butyl acrylate-based copolymers of variable composition and structure (statistical, diblock or triblock) was studied in solution at different temperatures and concentrations with turbidimetry measurements, differential scanning calorimetry, electronic microscopy, rheology and scattering experiments.

Findings: This study illustrates how it is possible through chemical engineering of the microstructure of amphiphilic thermoresponsive polymers to modulate significantly the self-assembly, morphological and mechanical properties of these materials in aqueous media. Statistical structures induced a strong decrease of cloud point temperature compared to block structures with similar composition. Moreover, block structures lead below the transition temperature to the formation of colloidal structures. Above the transition temperature, the formation of colloidal aggregates is observed at low concentrations, and at higher concentrations the formation of gels. Neutron scattering and light scattering measurements show that for a given composition diblock structures lead to smaller colloids and mesoglobules than their triblock counterparts. Moreover, diblock structures, compared to triblock analogs, allow the formation of gels that do not demix with time (no synaeresis) but that are softer than triblock gels.

KEYWORDS: thermoresponsive polymers, microstructure, RAFT, colloids, mesoglobules, hydrogel.

1. Introduction

Synthetic materials capable of responding in a controllable and predictable fashion to small changes in their environment (temperature, pH, mechanical stress…) have aroused great interest in the last decades. This response induces changes in the properties of these materials such as dimensions, internal structure or aggregation state.[1] In that context, thermosensitive systems, obtained by dissolving a polymer in aqueous solutions, have been extensively studied. They present a characteristic transition temperature called cloud point temperature (Tc) at which the interactions between the polymer chains and the aqueous media dramatically changed. This results in the collapse or expansion of polymer chains. If, in the phase diagram, a change from a two-phase to a single-phase system is observed when the temperature is increased, an upper critical solution temperature (UCST) is define. In the opposite case, a lower critical solution temperature can be defined (LCST). Among all polymers presenting a LCST, like poly(N-vinylcaprolactam) (PVCL),[2,3] poly(oligo(ethylene glycol) methacrylate),[4] etc.., poly(*N*-isopropylacrylamide) (PNIPAM) is by far the most commonly described.[5,6] Their thermoresponsive properties are used in nanoreactors, in stimuli responsive drug nanocarriers or to obtain surfaces with tunable hydrophobicity.[2,7-9] Interestingly, the choice of the macromolecular parameters of a chosen polymer (composition, molar mass, architecture…) greatly influences the properties of the obtained materials. Hence, whereas the cloud point temperatures T_c remained almost constant whatever the molar mass is in the case of PNIPAM,[2] this temperature can be precisely controlled by the adjustment of $\overline{M}_n$ in the case of PVCL with values tending to increase with the decrease of copolymer chain length. A strong, concentration-dependent polymer–solvent interaction is mainly responsible for this behaviour in the case of PNIPAM. Polymer architecture (linear, branched, hyperbranched, grafted…) also influences thermoresponsiveness of those polymers. Hence, four-arm PNIPAM stars collapse to form denser globules than the ones observed for linear PNIPAM[10] and PNIPAM-based branched thermoresponsive gel do not show the same kinetics of hydration and rheological properties than their linear counterparts.[11,12] Incorporation of hydrophilic comonomers within random or block copolymers enables to finely tune

LCST values:[13] random copolymerization with a 82/18 mol.% ratio of NIPAM with hydrophilic acrylamide monomer increase T_c value from 32°C to 45°C.[14] Similarly, random copolymerization of VCL with hydrophilic, N-vinyl formamide, N-methyl-N-vinylacetamide or vinylpyrrolidone (VP), induced a significant increase of T_c.[15,16] Thus copolymerization appears to be an effective means of modulating T_c even if, in most cases, this variation does not depend linearly on the comonomer ratio.[15] Moreover, this incorporation can lead to a rapid loss of heat-sensitive properties.[15,16] On the contrary, the incorporation of a hydrophobic monomer tends to decrease the observed transition temperature. Thus, statistical copolymerization of NIPAM with hydrophobic acrolein using a 80/20 mol.% ratio induced a decrease of T_c value down to 26°C.[14] A similar tendency is observed with block copolymers. In addition, below T_c, their specific microstructure confers an amphiphilic character to this block structure. This results in the formation of self-assemblies such as micellar structures or polymersomes.[13] Above T_c, the dehydration of the thermoresponsive block induces aggregation of the preformed nanoobjects.

In this article, copolymers of NIPAM and hydrophobic n-butyl acrylate (BA) monomer will be considered. Whereas this family of copolymers can act as stabilizers for nanoparticles[13] or emulsion systems,[17] few studies have described their properties in aqueous solution yet.[13,17-20] For instance, P(BA-*s*-NIPAM) statistical copolymers have been used to form hydrogels for which a decrease of T_c from 34.3 to 29.5°C was observed when BA content increased up to 20 mol.%.[21] The specific structure of PBA-*b*-PNIPAM block copolymer enabled the formation of stable nanospheres both below and above T_c [13, 19] with a significant increase of diameter above T_c.[13] Here, we aimed at further studying the properties of this family of copolymers at different temperatures and concentrations solution in relation with their composition and microstructure. For this, polymers with statistical, diblock and triblock microstructures were synthesized by reversible addition-fragmentation chain transfer (RAFT)/macromolecular design by interchange of xanthates (MADIX) copolymerization of NIPAM and BA[13,17]. The ability of the different copolymer structures to associate as colloids in dilute solution and to form gels at higher concentration, and the temperature dependence of these properties was studied with turbidimetry measurements, differential scanning calorimetry, electronic microscopy, rheology and scattering experiments.

2. Materials and Methods

2.1. Reagents

Ethyl xanthic acid potassium salt (97+%), *n*-butyl acrylate (99%) and n-isopropylacrylamide (99%) were supplied from Acros Organics. NIPAM was purified by recrystallization using a toluene: hexane (1:10 weight ratio) mixed solvent. Ethyl xanthic acid potassium salt and diethyl 2,5-dibromoadipate (Sigma-Aldrich, 98%) were used as received. 2,2'-azobis(2-methylproprionitrile) (AIBN, 98%) was purchased from Janssen Chimica and recrystallized from ethanol before use. Absolute ethanol (AnalaR Normapur VWR) was used as received. Water was purified thanks to an ion exchange resin (Purite device, resistivity ≈ 18 MΩ.cm). The *O*-ethyl-*S*-(1-methoxycarbonyl)ethyl dithiocarbonate (xanthate **X1**) RAFT/MADIX agent was synthesized according to an earlier procedure from our group.[22] The synthesis of meso-2,5-di(O-ethyl xanthate) diethyladipate (*bis*-xanthate **X2**) and of P(BA-*s*-NIPAM) statistical, PBA-*b*-PNIPAM diblock and PNIPAM-*b*-PBA-*b*-PNIPAM triblock copolymers with a theoretical $\overline{M}_n$ = 10000 g·mol^{-1} is described in supporting information.

2.2. Characterization

2.2.1. Characterization of synthesized polymers. ^1H and ^{13}C NMR spectra were recorded on a Bruker ARX 400 at 400.13 MHz and at 100.61 MHz, respectively. Number-average molecular weights ($\overline{M}_n$) and dispersities (Đ) of P(BA-NIPAM) copolymers were determined by size exclusion chromatography (SEC) on an apparatus equipped with a multi-angle light scattering (MALS) detector MiniDawn TREOS (Wyatt Technology Corporation) and a Waters 2140 refractive index (RI) detector using a Waters Styragel HR 4E column (eluent: THF; concentration 10 mg·mL^{-1}; flow rate: 1 mL·min^{-1}). Molecular weights were calculated based on RI-MALS detection. The value of dn/dC for block copolymers were calculated by using the measured values of homopolymer weighted by the composition of the measured copolymer. PNIPAM homopolymers samples were analyzed in DMF/LiCl (10 mmol·L^{-1}) as previously described.[13]

The thermal properties of the copolymers (in bulk and in solution) were determined by Differential Scanning Calorimetry (DSC) using a Mettler Toledo DSC 1 STARe System Thermal Analysis calorimeter equipped with a Gas Controller GC200. Glass transition temperatures were determined on heating at a heating rate of 10 °C·min^{-1}.

2.2.2. Determination of cloud points. All polymer concentrations were calculated as % weight/weight (w/w). For polymer solutions, cloud point temperatures were determined by using DSC measurements on 1, 5 and 20 wt.% sample solutions. Solution samples were sealed in impermeable crucibles of 120 µL. Cloud point temperatures, T_c, were estimated at the top of DSC while temperature decreased/increased at different rates; 20, 10, 5, and 1 °C·min^{-1}, and finally extrapolated to 0 °C·min^{-1}. The variation of enthalpy was measured as the temperature increased at a rate of 1 °C·min^{-1}. Transmittance of polymer aqueous solutions was recorded at 500 nm and different temperature with a Cary 100 Bio spectrophotometer at different heating/cooling rates (0.5, 1, 2.5 and 5 °C·min^{-1}). Cloud point temperatures were calculated from the determination of inflexion point of each transmittance curve, extrapolated to 0 °C·min^{-1}.

2.2.3. Characterization methods of colloids.

For Transmission Electron Microscopy (TEM) measurements, a drop of solution was placed on a formvar carbon-coated copper TEM grid (200 mesh, Ted Pella Inc.) and left to dry at the chosen temperature. The samples were viewed with a Hitachi HT7700 transmission electron microscope operating at 80 kV accelerating voltage. The size distribution of the particles was determined using WCIF Image J software and confidence intervals were given as average diameter ± standard deviation. An aqueous solution of uranyl acetate (2 wt.%, 2 min) was used for negative staining. NP size was determined via *Dynamic Light Scattering measurements* (DLS) using a Zetasizer Nano-ZS (Malvern Instruments, France). The reported apparent equivalent hydrodynamic diameter, D_h, is obtained by analyzing measured correlation function (on 5 different samples) via non-negative least square algorithm and using the Stokes–Einstein equation.

The analysis of polymer solutions at 20 °C and 40 °C by *Small Angle Neutron Scattering* (SANS) was carried out in D_2O at the Orphée reactor (LLB, Saclay) with PACE spectrometer as previously described.[13] Three configurations of neutron wavelength and distances were used to reach low, intermediate and high q values: 17Å/4.8m, 7Å/3m and 7Å/1m respectively. The measured scattering vector range was thus $0.0025 < q\ (Å^{-1}) < 0.35$. Neutron wavelength distribution $\Delta\lambda/\lambda$ is equal to 0.11. The efficiency of detector cells was taken into account by normalizing the scattered intensities by the incoherent signal delivered by a 1 mm gap water sample. The direct determination of the number of neutrons in the incident beam and the detector cell solid angle allow to obtain absolute values of the scattering intensity, I(q) in cm^{-1}.[24] The scattering curves of diluted copolymer solutions have been fitted using SASView software (http://sasview.org) to the model of polydisperse sphere (radius R) using a Gaussian distribution of radius (σ_R). For triblock at 20 °C, the best fit radii were very small (3 nm) and the distribution very large ($\sigma_R \sim$ 2-3). So curves of triblock at 20 °C were also fitted to the model of polydisperse sphere but with a log-normal distribution (an asymmetric distribution compared to the Gaussian one) in order to obtain more reasonable values of fit parameters.

2.2.4. Hydrogel characterization. Cryo-Scanning Electron Microscopy was performed with a FEG FEI Quanta 250 microscope (Japan). One drop of polymer solution was preheated to undergo gel transition just before being frozen in nitrogen slush at -220°C. The frozen sample was then fractured at -145°C in the cryo-fracture apparatus chamber under vacuum. After a sublimation step at -95°C during 30 min the sample was introduced into the microscope chamber at -145°C operating at a 5 kV accelerating voltage. Rheological measurements were made with an AR1000 rheometer from TA instruments in cone plate configuration (diameter 2 cm, 2° angle) equipped with a Peltier plate. An oscillatory stress with an amplitude of 1 Pa and at a frequency of 1 Hz was applied to the sample for viscoelastic measurements. With these settings, the variation of the elastic modulus G' and viscous modulus G" with temperature were

monitored, by applying a continuous linear temperature ramp at 1 °C·min^{-1}. The inflexion point was selected as the "transition temperature".

3. Results and discussion

3.1. Synthesis and characterization of copolymers.

In order to study the influence of copolymer composition and architecture on the thermoresponsive properties, three families of copolymers were investigated: P(BA-*s*-PNIPAM) statistical copolymers, PBA-*b*-PNIPAM diblock copolymers and PNIPAM-*b*-PBA-*b*-PNIPAM triblock copolymers. For each one of them, a similar $\bar{M}_n$ value of 10 000 g·mol^{-1} (abreviated as 10k) was selected.

Well-defined triblock copolymers comprising thermosensitive PNIPAM and PBA blocks were synthesized by RAFT/MADIX polymerization using *bis*-xanthate agent **X2** (**Scheme 1**). These block copolymers were synthesized via two-step polymerizations initiated by 2,2'-azobis(isobutyronitrile) in ethanol at 62°C without purification of the intermediate PBA block (**Scheme 1**).

PNIPAM-*b*-PBA-*b*-PNIPAM copolymers with targeted structures corresponding to PNIPAM$_{4k}$-*b*-PBA$_{2k}$-*b*-PNIPAM$_{4k}$, PNIPAM$_{2.5k}$-*b*-PBA$_{5k}$-*b*-PNIPAM$_{2.5k}$ and PNIPAM$_{1k}$-*b*-PBA$_{8k}$-*b*-PNIPAM$_{1k}$ were selected. In the conditions used, BA and NIPAM conversions were greater than 97% for each polymerization step and for all block copolymers. Next, diblock copolymers were obtained in a similar way in the presence of xanthate **X1** as previously described.[13] Three P(BA-s-PNIPAM) statistical copolymers: P(BA-*s*-NIPAM)$_{10k}$ (0.2:0.8 w), P(BA-*s*-NIPAM)$_{10k}$ (0.1:0.9 w) P(BA-*s*-NIPAM)$_{10k}$ (0.05:0.95 w) with similar molecular weights and different BA/NIPAM ratios were also synthesized. The list of all prepared materials and their macromolecular characteristics are given in **Table 1**.

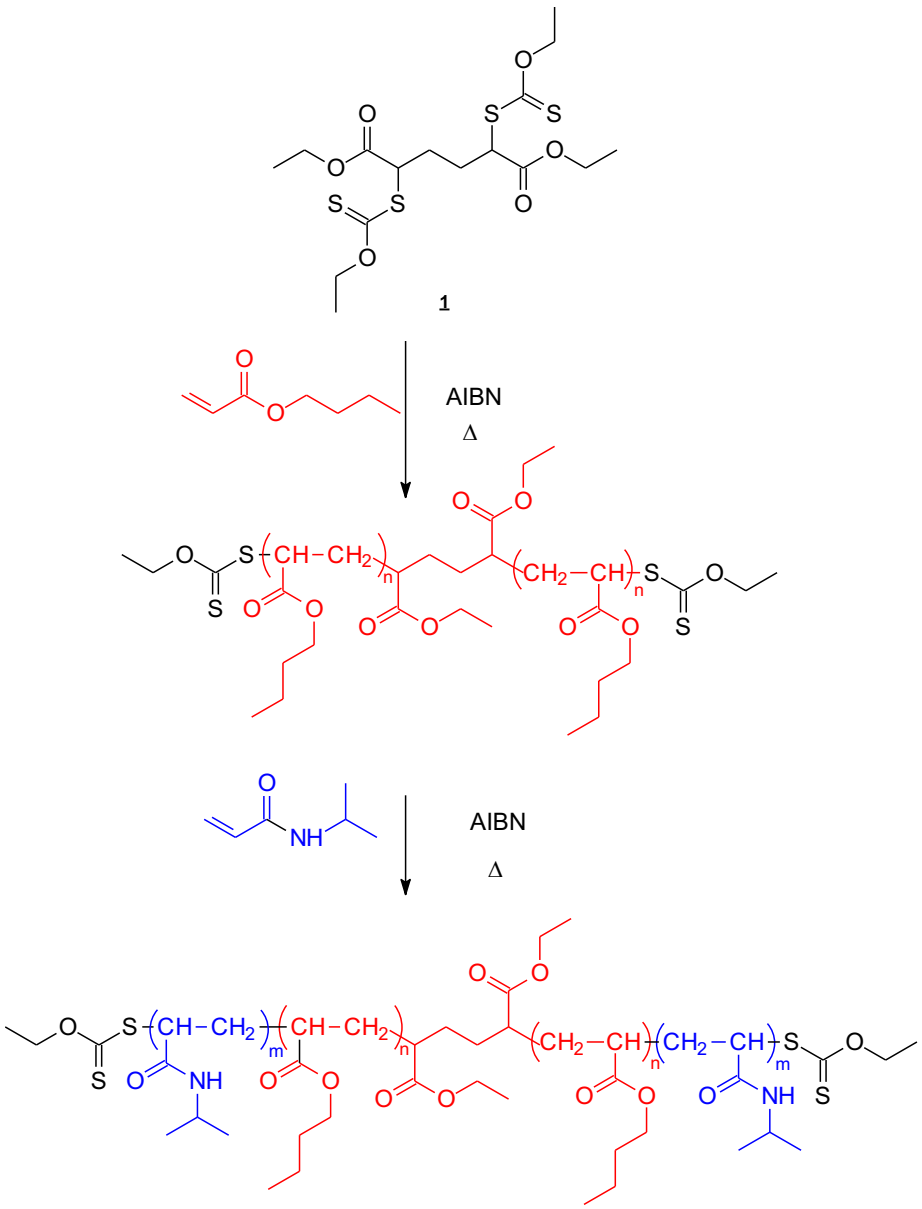

Scheme 1. Synthesis of PNIPAM-*b*-PBA-*b*-PNIPAM copolymers by RAFT/MADIX polymerization.

Table 1. Characteristics of various copolymers prepared by RAFT/MADIX polymerization: $\bar{M}_n$, dispersities (Đ) and glass transition temperatures (T_g).

PBA /PNIPAM	Sample	$\bar{M}_n$ (g·mol^{-1})[a]	$Đ$ [a]	T_g [b] (°C)	ΔC_p [b] (J·g^{-1}.K^{-1})
0.5k/9.5k	P(BA-*s*-NIPAM)$_{10k}$ (0.05:0.95 w)	10620	1.30	111.90	0.74
1k/9k	P(BA-*s*-NIPAM)$_{10k}$ (0.1:0.9 w)	11230	1.57	114.20	0.71
2k/8k	PBA$_{2k}$-*b*-PNIPAM$_{8k}$	10000	1.16	108.90	0.20
	P(BA-*s*-NIPAM)$_{10k}$ (0.2:0.8 w)	9100	1.81	100.40	0.63
	PNIPAM$_{4k}$-*b*-PBA$_{2k}$-*b*-PNIPAM$_{4k}$	8960	1.40	100.60	0.28
5k/5k	PBA$_{5k}$-*b*-PNIPAM$_{5k}$	9400	1.25	-48.00 106.70	0.10 0.20
	PNIPAM$_{2.5k}$-*b*-PBA$_{5k}$-*b*-PNIPAM$_{2.5k}$	11000	1.23	-35.20 86.21	0.10 0.28
8k/2k	PBA$_{8k}$-*b*-PNIPAM$_{2k}$	10100	1.20	-44.00 133.00	0.40 0.10
	PNIPAM$_{1k}$ -b-PBA$_{8k}$-*b*-PNIPAM$_{1k}$	9900	1.36	-41.70	0.56
PBA	PBA$_{2k}$	2400	1.38	-50.70	0.50
	PBA$_{5k}$	5750	1.35	-50.60	0.50
	PBA$_{8k}$	9500	1.30	-50.70	0.50
PNIPAM	PNIPAM$_{8k}$	17600	1.27	127.90	0.40
	PNIPAM$_{10k}$	21300	1.31	126.20	0.46

[a] SEC was performed in THF with RI-MALS detection expect in the case o f PNIPAM homopolymers for which SEC was performed in DMF/LiBr (10 mmol·L^{-1}) with PMMA calibration (40 °C, flow rate: 1mL·min^{-1}). In the latter case the chosen conditions led to an overestimate the given mass by a factor of two. [b] Glass transitions measured at a heating rate of 10°C·min^{-1}.

Number-average molecular weights ($\bar{M}_n$) and dispersities ($Đ$) were first determined by SEC (**Figures S9-S11** in ESI). It appears from the data reported in Table 1 that for all PBA precursors and BA/NIPAM copolymers, ($\bar{M}_n$) values are very close to theoretical expectations for a controlled RAFT/MADIX polymerization, which is in agreement with known values of transfer constants C_{tr} of BA and NIPAM to xanthate X1 ($C_{tr,X1}$=2.7[25] and 3.3[26] for BA and NIPAM in ethanol, respectively). The $\bar{M}_n$ of PNIPAM synthesized in the presence of X1 or X2 were nearly twice as high as the theoretical $\bar{M}_n$ value when SEC

was performed in DMF. We attributed these differences in $\bar{M}_n$ to differences in hydrodynamic volumes between PMMA and PNIPAM in the DMF/LiBr eluent, as the $C_{tr,X1}$ value of 3.3 for NIPAM rules out the possibility for the xanthate to be partially reacted at the end of the polymerization. As reported in **Table 1**, the dispersity values are close to 1.3 for PNIPAM and lie in the 1.3-1.4 range for PBA. By approximating at the end of the polymerization process $Đ$ to $1+1/C_{ex}$ (with C_{ex}=interchain transfer constant),[27] the xanthate exchange can be considered as relatively slow in both cases (C_{ex}~3 in line with $C_{tr,X1}$ values) and slightly slower in the case of NA than for NIPAM. Concerning the copolymers, their experimental $\bar{M}_n$ values are very close to theoretical estimations. Dispersity values of the block copolymers tend to slightly decrease compared to that of the PBA block precursor ($1.16 < Đ < 1.40$). Most importantly, as illustrated in the case of $PNIPAM_{2.5k}$-*b*-PBA_{5k}-*b*-$PNIPAM_{2.5k}$, the overlay of SEC chromatograms in THF of the PBA precursor and resulting diblock or triblock copolymers show that in both cases, the PBA was successfully incorporated in the final copolymer (triblock **Figure 1**).

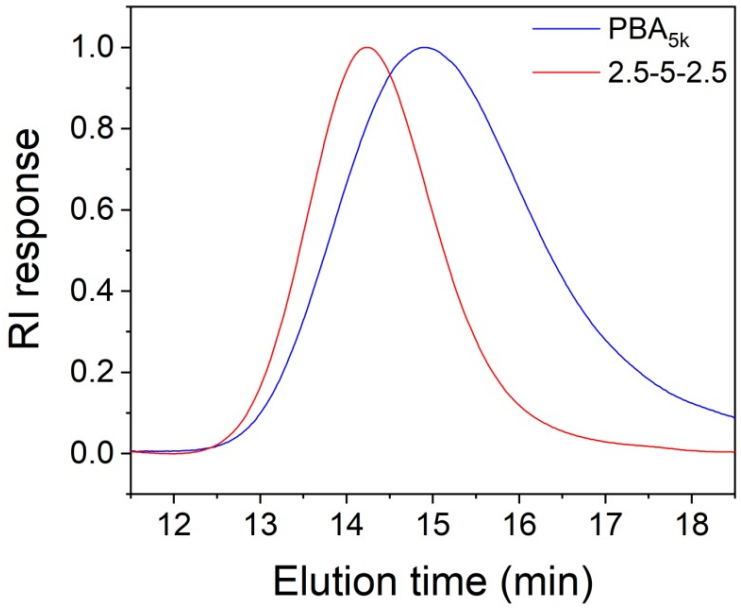

Figure 1. Size exclusion chromatograms (RI response) in THF of $PNIPAM_{2.5k}$-*b*-PBA_{5k}-*b*-$PNIPAM_{2.5k}$ (red line) and PBA_{5k} (blue line).

Thermal properties of block copolymers. DSC analysis was carried out for the different polymers (**Table 1**). As expected glass transition temperatures of statistical polymer decrease from 111.9 to 100,4°C when BA content increase from 5 to 20 wt.% within the polymer (see **Table 1**). Whereas block polymers with a 50/50 weight composition showed two glass transitions temperatures (around –50 and 100 °C), 2k/8k polymers presented only one around 100 °C. In the latter case, the lower weight fraction of PBA within the polymer prevents the possibility to see the transition corresponding to this block. Interestingly, the observed T_g values for triblock copolymers were found at lower temperature than the one observed for corresponding diblock or statistical copolymers. This suggests a different phase separation of the two blocks in the solid state.

3.2. Cloud points

In order to evaluate the influence of composition and microstructure on cloud point temperatures (T_c), the behavior of polymer solutions was studied as a function of temperature for concentrations ranging from 0.1 to 20 wt.%. Among the synthesized polymers, only those with a minimum PNIPAM content of 50 wt.% make it possible to obtain perfectly clear, i.e. soluble, solutions at room temperature. Subsequently, they will be the only ones whose behavior in solution will be studied by turbidimetry, DLS and DSC measurements. **Figure 2** gives a typical example of these measurements in the case of a 0.1 wt.% solution of $PNIPAM_{4k}$-*b*-PBA_{2k}-*b*-$PNIPAM_{4k}$ (for the other polymers, see **Figures S12-S17** in ESI). It has to be noted that for most polymers, there is no significant difference in the T_c values measured at different concentrations. Only PNIPAM shows a significantly different value at 0.1 wt.% compared to the values assessed at 5 and 10 wt.% (36, 32 and 32 °C respectively).

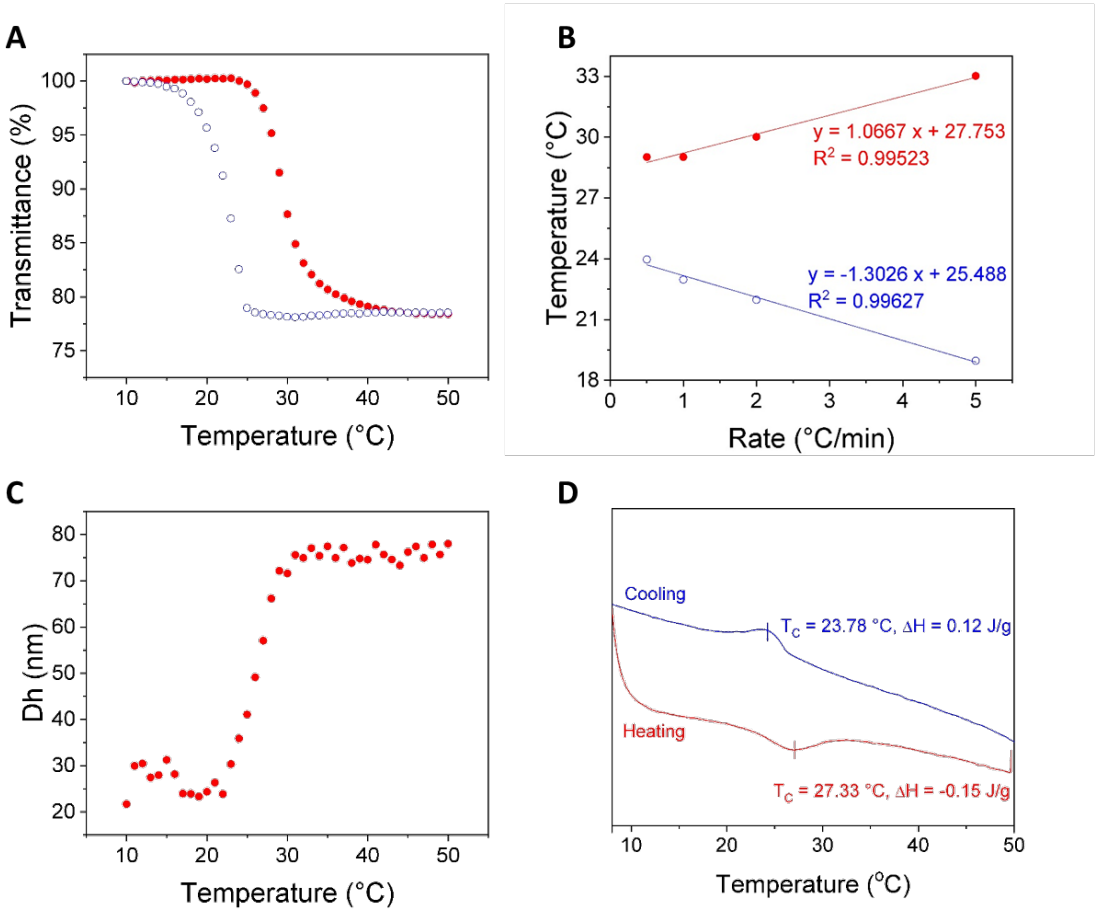

Figure 2. Turbidimetry (A and B), DLS (C) and DSC (D) measurements of a 0.1 wt.% (or 1 wt.% for DSC) aqueous solutions of $PNIPAM_{4k}$-*b*-PBA_{2k}-*b*-$PNIPAM_{4k}$ triblock copolymer. A) Transmittance monitored at 500 nm on heating and cooling (1 °C·min^{-1}). B) Extrapolation of measured inflexion points determine from turbidimetry curves at different heating/cooling rates. C) Hydrodynamic diameter obtained from DLS measurements on heating. D) DSC thermograms recorded on heating and cooling at the rate of 1 °C·min^{-1}.

Whatever the technique used, a sharp and reversible phase transition was observed. In addition, when comparing the behavior of polymer solutions while cooling or heating, a hysteresis phenomenon whose amplitude depends on the chosen heating/cooling rate is observed. This phenomenon is related to the difficulty of swelling compact aggregates formed at higher temperatures due to intra-chain entanglement.[28] Cloud point temperatures were evaluated from these measurements as detailed in the

experimental section. Hence, in the case of PNIPAM$_{4k}$-*b*-PBA$_{2k}$-*b*-PNIPAM$_{4k}$ T_c values equal to 27.7, 26.0 and 26.0 °C were obtained on heating thanks to turbidimetry, DLS and DSC measurements respectively. It should be noted that for these polymers of low molecular weight, the study of thermal properties with use of UV leads to a systematic overestimation of T_c values compared to those obtained from DSC or DLS measurements, regardless of the studied polymer family. Such effects can be attributed to the need for these techniques to obtain aggregates of sufficient size to be detectable. Thus, even as the dehydration of the polymer chain begins, as evidenced by DSC measurements, the formation of aggregates of sufficient size able to scatter light at a sufficient level requires a certain amount of time and/or greater dehydration level. Cloud point temperature (T_c) obtained by visual assessment DSC, DLS and turbidimetry measurements of aqueous solutions of the other polymers are given in **Table S3** in ESI. Therefore, DSC was performed on the different families of polymer in order to compare their T_c values and corresponding enthalpy variations (ΔH). **Figure 3** shows T_c values obtained on heating or cooling for the different families of polymer at a concentration of 1 wt.% (see **Table S4** and **Figure S18** in ESI for results obtained at 5 wt.% and 20 wt.%).

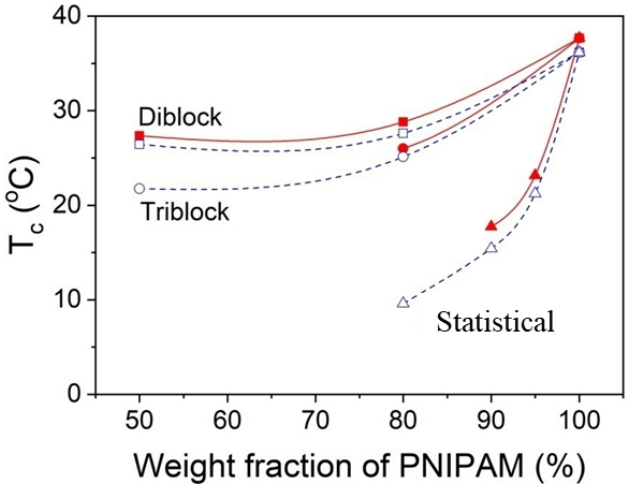

Figure 3. Cloud point temperatures T_c (peak maximum) obtained by DSC on heating (red plain marks) or cooling (blue open marks) for PNIPAM homopolymer and statistical, diblock and triblock PNIPAM-based copolymers at a concentration of 1 wt.%.

As can be seen in **Figure 3**, compared to PNIPAM homopolymer, incorporation of a hydrophobic monomer in the PNIPAM chain led to a significant decrease in the cloud temperature regardless of the considered structure, *i.e.* diblock, triblock or statistical. This trend is expected, as insertion of a hydrophobic moiety significantly decreases the level of hydration of polymer chain and thus decreases the cloud point temperature. At the same time, the measured enthalpy variations reported for a constant amount of PNIPAM decreased significantly when the amount of PNIPAM decreased. Hence, in the case of statistical copolymers, ΔH values equal to 31.58, 13.33 and 2.25 J per gram of PNIPAM were reported for a PBA content of 5, 10 and 20 wt.% respectively. Similar trends were observed for diblock and triblock copolymers but, as expected, to a lesser extent. Indeed, for these copolymers, disruption of hydrogen bond network is less expected due to the presence of large blocks of PNIPAM. In addition to this composition effect, the effect of the microstructure is highly pronounced. Hence, for a given composition (*i.e.* 80 wt.% of PNIPAM), the cloud point temperature measured for a random copolymer is well below the one measured for triblock and diblock structures (*i.e.* 9.62, 25.13 and 27.60 °C, respectively). In the case of a statistical copolymer, its specific microstructure seems to strongly disadvantage the hydration of the polymer. It also does not enable to study copolymers containing PBA fractions greater than 20 wt.%. Lastly, the slightly lower values of T_c for triblock structures compared to diblock ones might be related to a similar phenomenon: indeed, for a given composition, triblock structures present one supplementary transition between PBA and PNIPAM blocks.

3.3. Properties of Dilute Aqueous Solutions of Diblock and Triblock Copolymers.

In addition to effects on cloud point temperature, the microstructure also strongly impacts the solubility of the different studied polymers. Hence copolymers with a random structure present a low solubility in aqueous solutions (limited to 1 wt.%), whereas diblock and triblock copolymers thanks to their specific amphiphilic structure enable to obtain clear solution for weight ration up to 20 wt.%. This observation might be related to the formation of nanometric colloidal suspensions and will be studied in the following section.

3.3.1. Behavior below T_c

As evidenced by DLS measurements, in THF, block polymers behave as isolated chains at a concentration of 0.1 wt. %. When they were transferred from organic solvent into aqueous solutions, a significant increase of their hydrodynamic radii were observed by DLS whereas only a slight change was seen for the corresponding PNIPAM homopolymer (**Table 2**), suggesting that they have the ability to self-assemble. Additionally, TEM and SANS measurements were carried out to analyze the size and conformation as function of the copolymer architecture. All results are reported in **Table 2**.

Table 2. Cloud points (T_c) and DLS, TEM and SANS results on polymer aqueous solutions at 20 ºC and 40 ºC

Polymer	**Cloud point**	**Radius (nm) at 20 °C**			**Radius (nm) at 40 °C**		
	Tc[a]	$\langle R\rangle_{TEM}$	$\langle R_h\rangle_{DLS}$	$\langle R\rangle_{SANS}$	$\langle R\rangle_{TEM}$	$\langle R_h\rangle_{DLS}$	$\langle R\rangle_{SANS}$
$PNIPAM_{10k}$	32.3	-	3±2	-	-	243±97	-
PBA_{2k}-*b*-$PNIPAM_{8k}$	27.6	11.0±1.5	14±3	8±1	-	57±3	52±7
$PNIPAM_{4k}$-*b*-PBA_{2k}-*b*-$PNIPAM_{4k}$	25.1	10.6±2.3	10.5±2.0	4.9±2.0**	21.6±3.5	78±2	39±11
PBA_{5k}-*b*-$PNIPAM_{5k}$	26.4	20.5±5.0	31±6	20.5±3.5	-	66±1	53±8
$PNIPAM_{2.5k}$-*b*-PBA_{5k}-*b*-$PNIPAM_{2.5k}$	21.7		53.5±2.5	9±5**		123±2	46±7

[a] Obtained from DSC measurements (1 wt.% in cooling mode). Radius values are given for 0.1 wt.% polymer solutions. Preparation methods (direct solubilization, liposomes-like, …) do not influence Rh. Note: Errors in DLS results were calculated by multiplying polydispersity index values by the mean hydrodynamic radius values. Error in the fits results from SANS were calculated by multiplying the distribution by the radius values. ** log-normal distribution

For $PNIPAM_{4k}$-*b*-PBA_{2k}-*b*-$PNIPAM_{4k}$ a hydrodynamic radius equal to 10.5 ± 2.0 nm was measured. TEM images of dried aqueous solutions show very regular monodisperse spherical structures with average radius equal to 10.6 ± 2.3 nm (**Figure 4B**) in fair agreement with DLS results. This suggests the formation of spherical-like micellar structures for copolymer, as confirmed by SANS measurements shown in **Figure 4A**. Data were well fitted by a simple model of polydisperse spheres, which gave the mean micelle

radius and its Gaussian distribution (**Table 2**). In this case, the PNIPAM corona surrounding the PBA core is also swollen by the solvent. Its contribution to the SANS signal is very weak. Thus, with this assumption, the micelle radius deduced from SANS is the radius of the hydrophobic PBA core alone. The micelles radii of $PNIPAM_{2.5k}$-*b*-PBA_{5k}-*b*-$PNIPAM_{2.5k}$ copolymers measured by DLS and SANS are twice those of $PNIPAM_{4k}$-*b*-PBA_{2k}-*b*-$PNIPAM_{4k}$. Such an increase of micelle size related to the length of the hydrophobic block might be related to the strong aggregation limit case predicted and observed for the aggregation of diblock copolymer.[29] In this case, the hydrophobic blocks are mainly located in the core of the micelles. Longer hydrophobic block, led to the formation of micelles with a higher aggregation number and a larger micelle size. The average aggregation number N_{agg} of these micelles can be assessed from the following formula by considering a dense and solvent excluded core:

$$N_{agg} = 4\pi\rho_{core}R_{core}^{3}N_{av}/(3M_{core}) \quad (1)$$

with R_{core}: the radius of the core, M_{core}: the mean average molar mass of the core block which (here $M_{core} = M_{PBA}$), ρ_{core} =1.1 $g.cm^{-3}$: the block density of the core. From this, average aggregation number N_{agg} = 163 and 405 were found for copolymer micelles made of $PNIPAM_{4k}$-*b*-PBA_{2k}-*b*-$PNIPAM_{4k}$ and $PNIPAM_{2.5k}$-*b*-PBA_{5k}-*b*-$PNIPAM_{2.5k}$ respectively. By noting N_A the number of monomers of the hydrophobic block, the observed increase of N_{agg} is in good agreement with the expected scaling law $N_{agg} \propto N_A^2$.[29] The surface area per chain calculated from $A_c = 4\pi R_{core}^2 / N_{agg}$ gives values of 1.85 and 2.52 nm^2 respectively.

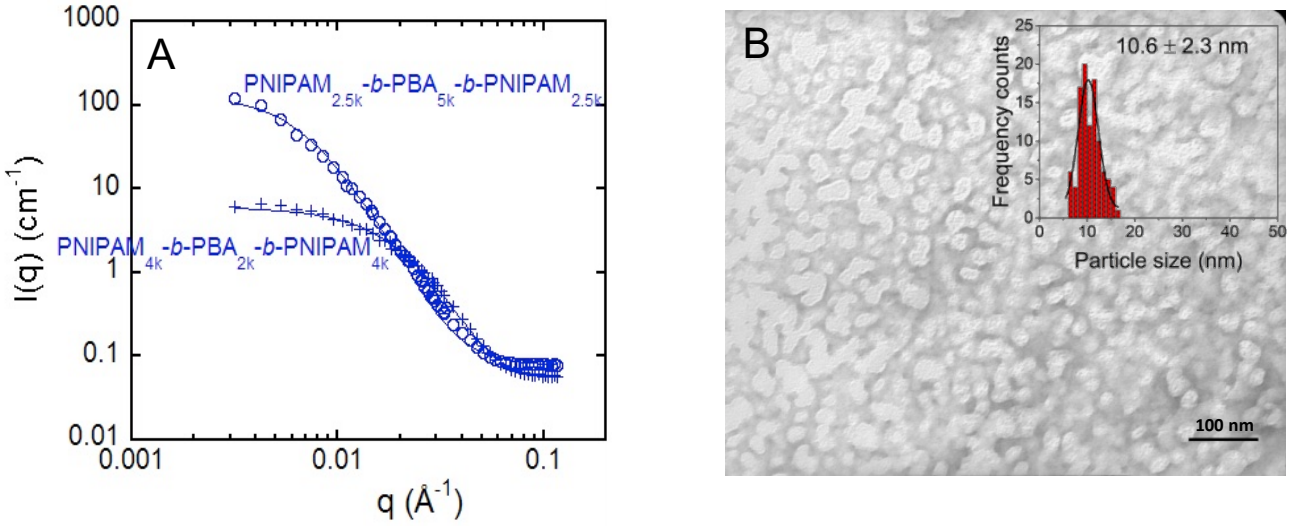

Figure 4. (A) Scattering intensity in absolute units (cm^{-1}) of D_2O solutions of (0.1 wt.%) $PNIPAM_{4k}$-*b*-PBA_{2k}-*b*-$PNIPAM_{4k}$ (+) and $PNIPAM_{2.5k}$-*b*-PBA_{5k}-*b*-$PNIPAM_{2.5k}$ (o) measured at 20 °C. Lines are the best fits to a model of polydisperse sphere with a log-normal distribution. (B) Representative TEM micrograph of aggregates formed by $PNIPAM_{4k}$-*b*-PBA_{2k}-*b*-$PNIPAM_{4k}$ at 20 °C stained with uranyl acetate (TEM deposit performed above T_c).

Diblock copolymers show the same tendency, i.e. an increase of size and aggregation number with an increase of PBA content[13] with N_{agg} = 710 and 4800 respectively for copolymer micelles from PBA_{2k}-*b*-$PNIPAM_{8k}$ and PBA_{5k}-*b*-$PNIPAM_{5k}$ with a surface area per chain in the corona for the two micellar systems gives values of 1.13 and 1.10 nm^2 respectively. Thus, at 20 °C, both diblock and triblock structures enable the formation of micellar structures. For a given composition, these specific structures favour their solubility and are responsible for higher T_c values compared to the statistical microstructure. In addition, compared to diblock copolymers, triblock counterparts led to smaller and less dense structures.

3.3.2. Self-Assembly in Water above the cloud point.

As shown in **Figure 5**, when a 0.1 wt.% solution of $PNIPAM_{4k}$-*b*-PBA_{2k}-*b*-$PNIPAM_{4k}$ was heated, hydrodynamic radii determined from DLS measurements evolved from 10 nm below T_c to 80 nm above T_c (**Table 2**). The formation of spherical aggregates with a narrow size distribution was further confirmed by TEM experiments (negative staining) and SANS measurements as shown in **Figure 5**. The estimated radius distribution from TEM measurements is equal to 21.6 ± 3.5 nm. The large distribution observed by TEM might be caused by drying and/or the staining process which leads to local overconcentration and, consequently, induces the formation of objects of different sizes. However, samples that were prepared using the same procedure at room temperature did not show such large objects (see **Figure 4B**). Since the aggregates appear to be spherical, it was consistent to fit the SANS data (see **Figure 5A**) above T_c with the polydisperse sphere model, which gave a mean radius of 39 ± 11 nm for $PNIPAM_{4k}$-*b*-PBA_{2k}-*b*-$PNIPAM_{4k}$. At this temperature, PNIPAM was poorly solvated and both blocks contribute to scattering signal. This behavior that induced the formation of large aggregates when the temperature is increased is observed whatever the structure and composition studied. Hence, from SANS measurements, $PNIPAM_{2.5k}$-b-PBA_{5k}-b-$PNIPAM_{2.5k}$ forms aggregates with a similar radius within experimental error (i.e. 46 ± 7 nm). Moreover, for diblocks, radii equal to 52 ± 7 nm and 53 ± 8 nm for PBA_{2k}-*b*-$PNIPAM_{8k}$ and PBA_{5k}-*b*-$PNIPAM_{5k}$ respectively. Thus, above T_c, these aggregates have similar size whatever the nature of microstructure (diblock or triblock). The formation of spherical aggregates also named mesoglobules has been previously described in the case of PNIPAM homopolymers[30, 31] as well as of hydrophobically-modified PNIPAM polymers[32] and PNIPAM-based amphiphilic block copolymers[13]. These mesoglobules are stable in solution and they spontaneously transform into spherical micelles when the solution was cooled below T_c: formation of larger aggregates was prevented by the low probability of Brownian collisions in dilute solutions.[30] Above T_c, polymer chains dehydrates and as a result intrachain contraction and interchain association occurred, giving rise to the formation of large aggregates poorly hydrated. Consecutively to the further ejection of water molecule to bulk water, very dense and rigid mesoglobules are formed. The probability of merging of different mesoglobules might be very low due

to both very short contact time between two mesoglobules during a collision or due to partial vitrification taking place within dense mesoglobules.[33]

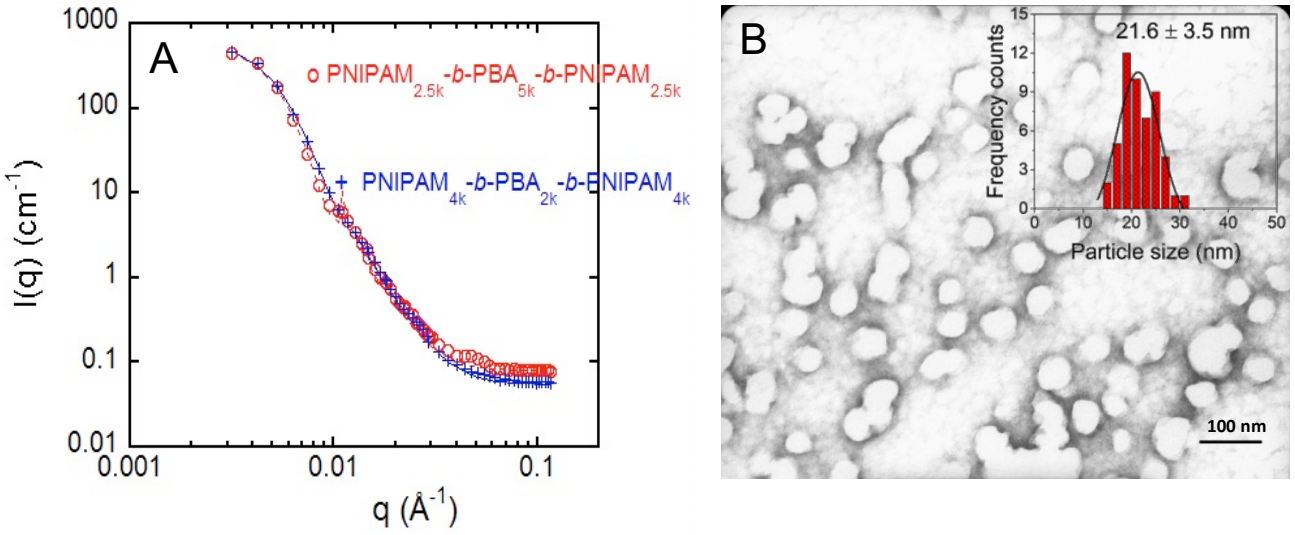

Figure 5. (A) Scattering intensity in absolute units (cm^{-1}) of D_2O solutions of (0.1 wt.%) $PNIPAM_{4k}$-*b*-PBA_{2k}-*b*-$PNIPAM_{4k}$ (+) and $PNIPAM_{2.5k}$-*b*-PBA_{5k}-*b*-$PNIPAM_{2.5k}$ (o) measured at 36 °C. Lines are the best fits to a model of polydisperse sphere with Gaussian distribution. (B) TEM image (negative staining) of aggregates formed above the cloud point for $PNIPAM_{4k}$-*b*-PBA_{2k}-*b*-$PNIPAM_{4k}$ (TEM deposit performed above T_c).

3.4. Formation and characterization of thermosensitive hydrogels

The behavior of polymer solutions for concentrations ranging from 0.1 to 20 wt.% was then studied. For this range of concentration, DSC measurements do not show significant changes in the measured transition temperatures T_c whatever the considered structures (diblock or triblock). Related enthalpy variation normalized with respect to PNIPAM content showed a strong decrease when the concentration increased. As such a decrease is not observed in dilute conditions, it tends to demonstrate a clear difference between the different polymers concerning the polymer/polymer and polymer/solvent interactions in gel solution. Interestingly, the concentration effect proves to have a strong impact on the rheological

properties of the studied solutions. An initial visual assessment of the effect of temperature for different polymer structures, compositions or concentrations was performed (**Figures S19-S22** in ESI). As an example, **Figure 6** shows photographs of the observed phase transition for PNIPAM$_{4k}$-*b*-PBA$_{2k}$-*b*-PNIPAM$_{4k}$ triblock structure at a concentration of 20 wt.%.

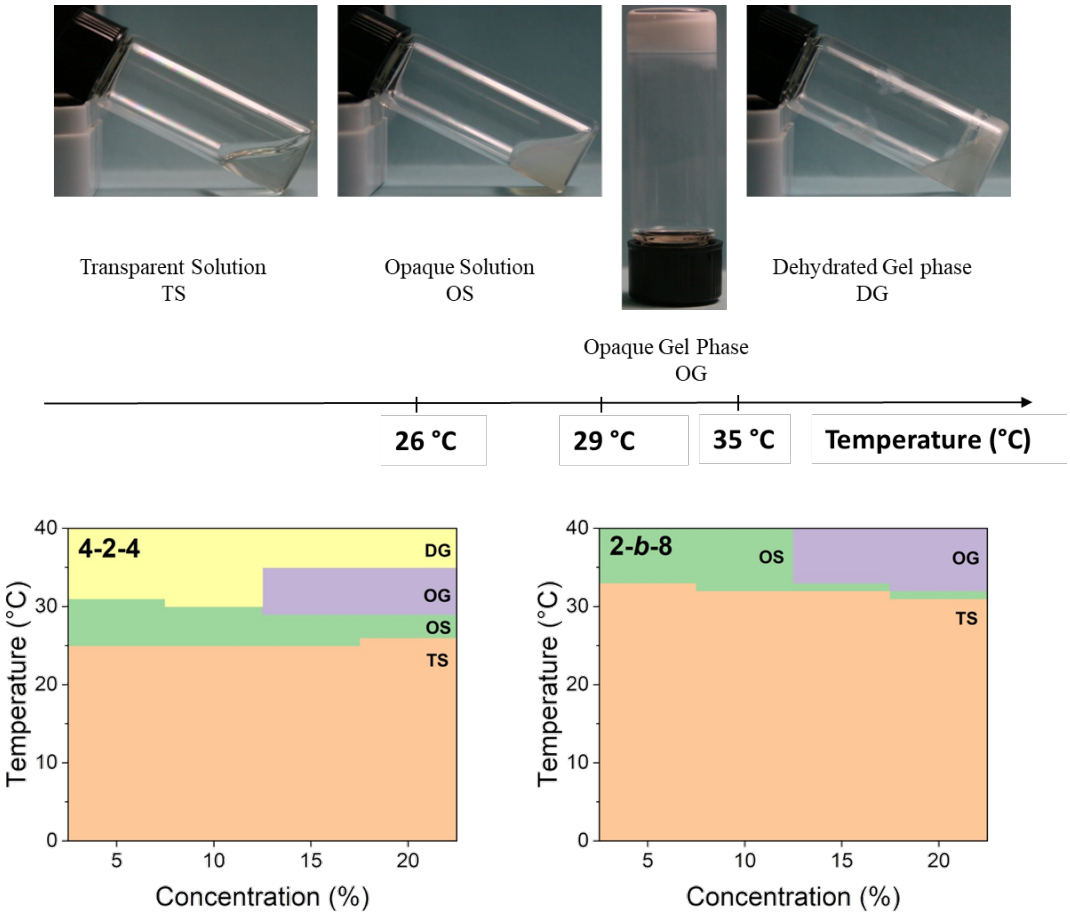

Figure 6. Photographs of the observed phase transition for PNIPAM$_{4k}$-*b*-PBA$_{2k}$-*b*-PNIPAM$_{4k}$ triblock structure at a concentration of 20 wt.% as function of temperature: Transparent Solution (TS phase)→ opaque solution (OS) → opaque gel phase (OG) → dehydrated gel phase (DG). Phase diagram of aqueous polymer solutions for PNIPAM$_{4k}$-*b*-PBA$_{2k}$-*b*-PNIPAM$_{4k}$ (left) and PBA$_{2k}$-*b*-PNIPAM$_{8k}$ (right) as a function of temperature and concentration.

Below T_c, i.e. 26 °C, the transparent polymer solution looked like a free-flowing liquid independently of the concentration so that we named this phase Transparent Solution (TS). As the solution was heated above the transition temperature, the solution rapidly became white and turbid but remained freely mobile.

This phase was noted OS as Opaque Solution. Then heating more, an opaque gel phase (OG) appeared: this gel phase was identified by gently tilting the vials[34] when no fluidity was visually observed on tilting after 5 min. As temperature was increased, macrophase separation occurred (synaeresis), with volume shrinkage by expelling water, and forms the final dehydrated gel phase (DG). Based on these measurements, a phase diagram describing the behavior of aqueous polymer solutions as a function of concentration was established (**Figure 6**) and compared to the ones of PBA_{2k}-*b*-$PNIPAM_{8k}$ diblock copolymer. Whereas for the homopolymer $PNIPAM_{10k}$, the formation of gel was only observed for the highest concentration of polymer used (i.e. 20 wt.%, see **Figures S21** and **23** in ESI), for the diblock and triblock structures gel formation occurred at lower concentrations (15 wt.% or lower). In all cases, those gelation concentrations were found to be much higher than the entanglement concentration which can be evaluated around 3 wt.% in the case of $PNIPAM_{10k}$.[35] Interestingly the synaeresis effect inducing the formation of dehydrated gel is strongly related to the chemical structure of the polymer. Whereas homopolymer and triblock copolymer present a pronounced synaeresis effect after only few minutes, diblock structure is less prone to demonstrate such an effect. Results from literature demonstrate also that gels obtained from branched or random structure favor the formation of gel without pronounced synaeresis effect.[15,12] In addition to the effect of structure, the effect of composition was also studied: hence triblock structures $PNIPAM_{2.5k}$-*b*-PBA_{5k}-*b*-$PNIPAM_{2.5k}$ with a higher PBA content favor the formation of gel at lower concentration, i.e. down to 5 wt.%, with a highly pronounced synaeresis effect (see **Figure S19** in ESI). This first set of experiments enables us to evidence the effect of microstructure on the macroscopic behavior of concentrated solution.

Rheological measurements provided a quantitative characterization of the mechanical changes during sol-gel transition. The elastic modulus G' and the viscous modulus G" were monitored from 20 to 31 °C for $PNIPAM_{4k}$-*b*-PBA_{2k}-*b*-$PNIPAM_{4k}$, and from 20 to 35°C for PBA_{2k}-*b*-$PNIPAM_{8k}$ with 1 °C·min^{-1} heating ramp. The maximal temperatures have been selected within the OG domain, so that the gels do not undergo synaeresis during the experiment. The oscillatory stress amplitude was set at 1 Pa and the

frequency at 1Hz (**Figure S24** in ESI). **Figure 7** shows the variation of G' and G" with temperature for 20 wt.% of aqueous solution of PNIPAM$_{4k}$-*b*-PBA$_{2k}$-*b*-PNIPAM$_{4k}$ and PBA$_{2k}$-*b*-PNIPAM$_{8k}$.

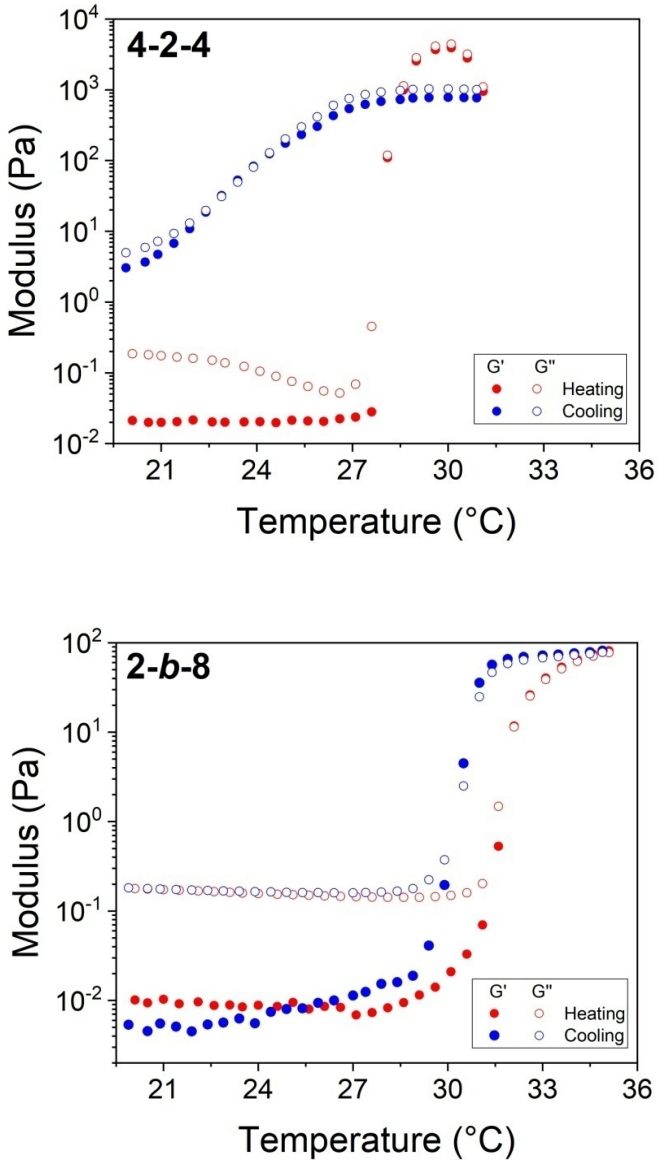

Figure 7. Temperature – dependent storage G' (empty marks) and loss G'' (filled marks) moduli for PNIPAM$_{4k}$-*b*-PBA$_{2k}$-*b*-PNIPAM$_{4k}$ and PBA$_{2k}$-*b*-PNIPAM$_{8k}$ (20 wt.% aqueous solutions) with heating rate at 1 °C·min^{-1}.

The sol-gel transition is observed at a temperature around 28 °C with a maximal modulus G' equal to 3000 Pa for PNIPAM$_{4k}$-*b*-PBA$_{2k}$-*b*-PNIPAM$_{4k}$ and 31.5 °C and 100 Pa for PBA$_{2k}$-*b*-PNIPAM$_{8k}$. The measured temperatures are found slightly higher than measured cloud point temperature from DSC measurements

(25.1 and 27.6 °C for triblock and diblock structures respectively). This might be ascribed to measurement conditions: for rheology measurements sample volume might induces inertia phenomenon and contrary to DSC measurements these values are not obtained by extrapolation of heating rate at $0°C \cdot min^{-1}$ (a heating rate of $1°C \cdot min^{-1}$ is used). Moreover a sufficient level of dehydration of the polymer is required in order to induce the formation of gel. Concerning the mechanical properties of the obtained gels, the stiffness of the gel obtained from the triblock structure is much higher than the one issued from diblock structure (G' equal to 3000 and 100 Pa respectively). These values were found significantly higher than the ones observed by for hydrogels made of 20 wt.% PNIPAM homopolymers, i.e. 20 Pa (see **Figure S25** in ESI).[12] Before the transition, typically G">G', while after the transition, G' becomes (slightly) higher than G" for both copolymers. In more detail, the measurement of G' and G" with a frequency sweep for the sol and the gel phases has been performed to determine the viscoelastic nature of these phases (see **Figure S26** in ESI).These measurements confirm the gel status for both triblock and diblock gels at 31 and 35°C, G' and G" being nearly independent of the frequency from 10 to 0.1 Hz. Conversely, at 20°C, when both copolymers preparations are liquid, G' and G" display a typical behavior of viscoelastic fluids that follow a Maxwell model: at low frequencies G' is proportional to $(f)^2$ and G" is proportional to f. G' and G" curves cross at a quite high frequency around 10 Hz, that gives an indication of the relaxation time of both polymer solutions, $\tau \approx 0{,}018$ s (triblock) and 0.015 s (diblock). A small hysteresis effect is observed for the diblock copolymer when cooling the solution back to room temperature. For the triblock copolymer, a more pronounced hysteresis effect was observed that could be related to the higher viscosity and relaxation time than with the diblock copolymer that could affect the mobility of polymer chains. Because of this large hysteresis, cycling the triblock polymer solution from 20 to 31°C gives a good reproducibility of the sol-gel transition temperature, but G' and G" values and cooling curves (gel-sol) are more variable (see **Figure S27** in ESI). The variability may also be related to the synaeresis effect observed with the triblock structure.

The properties of these hydrogels is likely to be strongly related to their internal structure. Thus, to gain insight into the network structure of the hydrogels, freeze-dried samples were analyzed with scanning electron microscopy at cryogenic temperature (cryo-SEM, **Figure 8**).

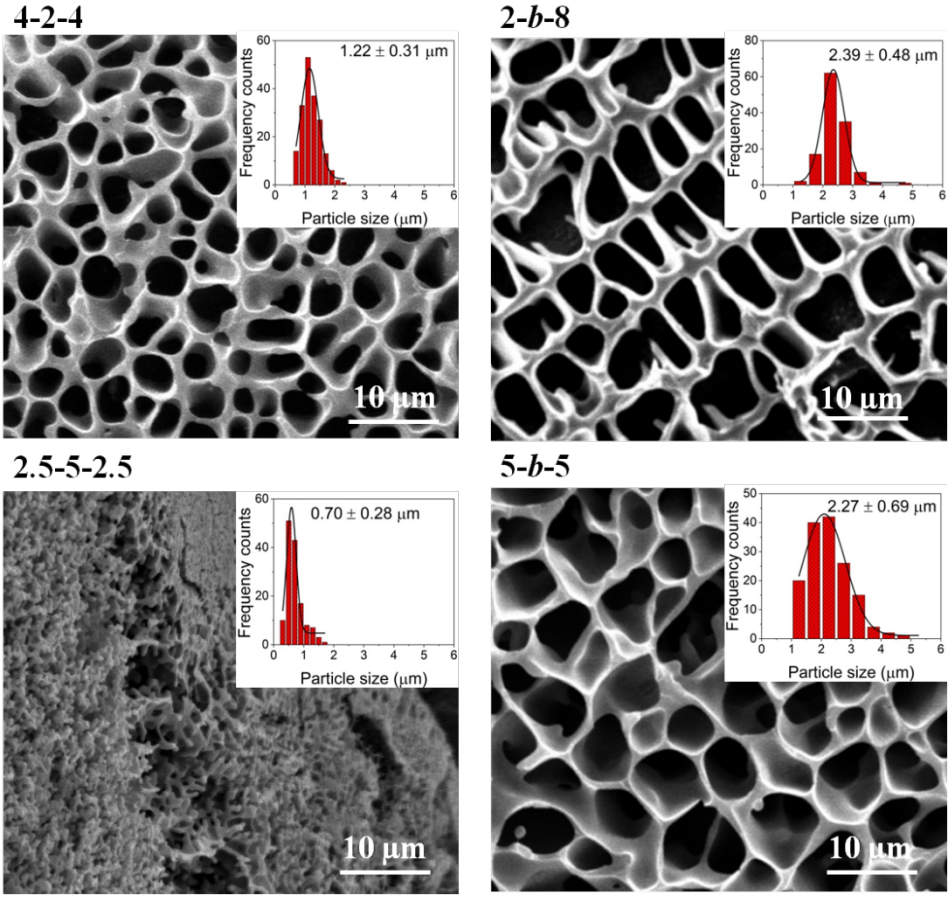

Figure 8. Images obtained from cryo-SEM of gel structures at 40 °C obtained from $PNIPAM_{4k}$-*b*-PBA_{2k}-*b*-$PNIPAM_{4k}$ (noted 4-2-4), PBA_{2k}-*b*-$PNIPAM_{8k}$ (noted 2-*b*-8), $PNIPAM_{2.5k}$-*b*-PBA_{5k}-*b*-$PNIPAM_{2.5k}$ (noted 2.5-5-2.5) and PBA_{5k}-*b*-$PNIPAM_{5k}$ (noted 5-*b*-5) (size distribution of pores are given as insets).

Thus, the study of concentrated polymer solutions makes it possible to highlight the crucial effect of the microstructure on macroscopic properties. For the same composition, the triblock structure leads to denser networks more likely to be the seat of important synaeresis and presenting slower rehydration kinetic.

The freeze-dried hydrogels show honeycomb-like microstructures with dense cell walls. Nevertheless, the cell/pore average size differs strongly, decreasing from the diblocks to the triblocks structure. Therefore, a clear relationship between molecular architecture and microstructure is evidenced: for a similar chemical composition, triblock structure promotes denser network structures with smaller pore size. A good correlation is observed between the increase of G' modulus and the apparent density of the gels. This difference of microstructure could also explain the differences observed on synaeresis effect between diblock and triblock structures, because network less dense might accomodate more easily the large volume of solvent.

3.5. Discussion

Numerous studies have in the past already compared the properties of polymers with different microstructures but similar compositions in solution. For instance, solutions of statistical and block copolymers present different rheological properties.[36,37] In the particular case of thermoresponsive polymers, branched and hyperbranched structures have been demonstrated to strongly affect the properties of PNIPAM-based polymers either in dilute conditions or in gel phase,[11,12] and block copolymers with a statistical structure present cloud point temperature more sensitive to their composition than block counterpart.[15,38] Through this study we compared for the first time in a systematic way the effect of composition and statistical, diblock and triblock microstructure on the properties in solution of amphiphilic thermoresponsive polymer at different concentrations and temperatures. The transition temperature of these copolymers in solution depends, as expected, on their composition: an increase of the fraction of hydrophobic part leads to a decrease of the transition temperature. This temperature also depends on the microstructure for a given composition: in comparison with block structures, the statistical structure is detrimental, as expected, to the good hydration of the hydrophilic monomers due to their microenvironment, thereby leading to a significant decrease in transition temperatures.

Below the transition temperature, block copolymers have an amphiphilic character, which led spontaneously to the formation of colloidal structures above a critical aggregation concentration (cac) as

illustrated in scheme 2. Their existence promotes the dispersability of these polymers in aqueous solution even at high concentrations. The structure of the objects formed depends in particular on the composition of the block copolymer and on the preparation method used.[39] Moreover the rate of exchange of polymer chains within these objects primarily depends on the interfacial tension between the hydrophobic block and water, the length of the hydrophobic block and architecture. Due to a too large interfacial tension, exchanges are absent for large hydrophobic blocks as observed in the case of BA-based copolymers which lead to kinetically frozen aggregates.[40] Hence different groups have reported that PBA-based amphiphilic block copolymers do not reorganize, or only very slowly, in spite of liquid like behavior of their hydrophobic blocks.[41-43] To induce faster exchange of polymer chains within these aggregates, copolymerization of hydrophilic units like acrylic acid in the PBA block can be used: it reduces the interfacial tension between the moderately hydrophobic block and the hydrophilic block and water.[44] Moreover, in the case of PBA-b-PNIPAM copolymers, the incorporation of dimethyl acrylamide hydrophilic units within PBA block hase shown to decrease the degree of hysteresis associated with the thermal transition.[20] All these results from literature suggested that, below T_c, PBA-*b*-PNIPAM diblock and PNIPAM-*b*-PBA-*b*-PNIPAM and triblock structures act as frozen micelles above a critical aggregation concentration. Also as demonstrated by DLS and SANS measurements and as discussed above in section 3.3, compared to diblock copolymers, triblock counterparts led to smaller and less dense frozen micellar structures with significantly lower aggregation number.

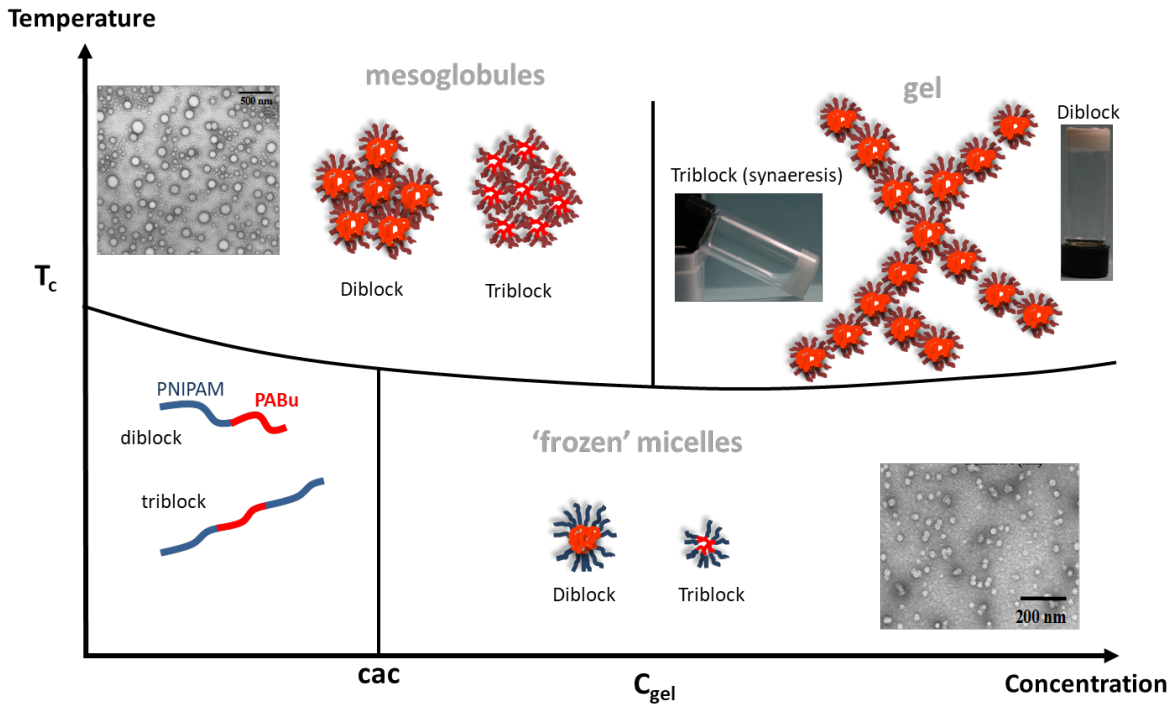

Scheme 2. Schematic behaviour of the diblock and triblock copolymers in solution as a function of concentration and temperature. For statistical copolymers, no micelle or gel were observed, only a transition towards a turbid solution above T_c.

Above the transition temperature and at low concentrations, for a chosen polymer structure, the formation of colloidal aggregates, i.e. mesoglobules, is observed. These nanoobjects are issued from the dehydration of PNIPAM corona of previously described micelles. The frozen PBA core prevents further reorganization of the polymer within and between the aggregates. Thus, by decreasing temperature above T_c, a fast hydration process of PNIPAM corona is possible. This mechanism enables a fast and reversible formation of so called mesoglobules from diblock and triblock structures. These aggregates have similar size whatever the nature of microstructure (diblock or triblock). At higher concentrations the formation of gels is observed (Scheme 2). Their formation might be related to the interconnection of dehydrated micelles in the whole solution when a sufficient concentration of nanoobjects is reached. Diblock structures, compared to triblock structures, allowed the formation of gels that are softer than triblock gels but that do not demix with time (no synaeresis). This might be ascribed to the ability of diblock structures to favour the formation of more efficiently interconnected network of dehydrated frozen micelles that

have less tendency to aggregate as demonstrated in the case of dilute solutions. Triblock structures compared to their diblock counterparts form stiffer and more viscous gels, with high syneresis and slower rehydration kinetics. These properties can be related to the nature of the hydrogen-bonded network, which is denser and therefore with smaller pores due to the reception of a smaller quantity of solvent.

4. Conclusions

The microstructural engineering of amphiphilic thermoresponsive copolymers of n-butyl acrylate and N-isopropylacrylamide allows significant modulations of the self-assembly, morphological and mechanical properties of these materials in aqueous media. With similar composition, the hydrophobic acrylate monomer in block copolymers contributes to a decrease of cloud point temperatures compared to pure PNIPAM to a much lesser extent compared to statistical structures, and enhances their solubility in aqueous solutions via self-assembly. In addition, below the cloud point temperature, block structures of appropriate composition lead to the formation of colloidal aggregates. Above this temperature, the formation of colloidal aggregates is observed at low concentrations, and gels are formed at higher concentrations. For a given composition, scattering experiments demonstrate that diblock structures lead to smaller colloids and mesoglobules than their triblock counterparts. Moreover, diblock copolymers lead to larger and more dense structures compared to triblock analogues and allow the formation of gels that do not demix with time (no synaeresis) but that are softer than triblock gels. While results in the literature have already demonstrated the important effect of architecture[11,12] or microstructure[36,37] on the properties of polymer solutions, the effect of microstructure on the properties of amphiphilic polymer assemblies has been more rarely reported .[44] Our study based on a thermosensitive polymer family also shows the striking effect of microstructure related to temperature on solution-generated organizations. Further studies will concern amphiphilic gradient copolymers[45] whose intermediate microstructure between block and statistical should enable to further modulate thermoresponsiveness of the polymers and obtain micellar aggregates with improved dynamics of assembly.

ACKNOWLEDGMENT. The authors acknowledge CSC Chinese government scholarship and EU for financial support (FEDER-35477: Nano-objets pour la biotechnologie). This work benefited from the use of the SasView application, originally developed under NSF Award DMR-0520547. SasView also contains code developed with funding from the EU Horizon 2020 programme under the SINE2020 project Grant No 654000.

References

[1] Gibson M. I., O'Reilly R. K., To aggregate, or not to aggregate? considerations in the design and application of polymeric thermally-responsive nanoparticles. Chem. Soc. Rev., 2013, 42:7204-7213. DOI: 10.1039/c3cs60035a.

[2] Beija M., Marty J. D., Destarac M., Thermoresponsive poly(N-vinyl caprolactam)-coated gold nanoparticles: sharp reversible response and easy tunability. Chem. Commun., 2011, 47:2826-2828. DOI: 10.1039/c0cc05184e.

[3] Liu J., Debuigne A., Detrembleur C., Jerome C., Poly(N-vinylcaprolactam): a thermoresponsive macromolecule with promising future in biomedical field. Adv. Healthc. Mater., 2014, 3:1941-1968. DOI: 10.1002/adhm.201400371.

[4] Lutz J. F., Akdemir O., Hoth A., Point by Point Comparison of Two Thermosensitive Polymers Exhibiting a Similar LCST: Is the Age of Poly(NIPAM) Over? J. Am. Chem. Soc., 2006, 128:13046-13047. DOI: 10.1021/ja065324n.

[5] Verdonck B., Goethals E. J., Du Prez F. E., Block Copolymers of Methyl Vinyl Ether and Isobutyl Vinyl Ether With Thermo-Adjustable Amphiphilic Properties. Macromol. Chem. Phys., 2003, 204:2090-2098. DOI: 10.1002/macp.200350069.

[6] Gan L. H., Gan Y. Y., Roshan Deen G., Poly(N-acryloyl-N'-propylpiperazine): A New Stimuli-Responsive Polymer. Macromolecules, 2000, 33:7893-7897. DOI: 10.1021/ma000928b.

[7] Brun Graeppi A. K. A. S., Richard C., Bessodes M., Scherman D., Merten O. W., Thermoresponsive surfaces for cell culture and enzyme-free cell detachment. Prog. Polym. Sci., 2010, 35:1311-1324.DOI:10.1016/j.progpolymsci.2010.07.007.

[8] Rzaev Z. M. O., Dinçer S., Pişkin E., Functional copolymers of N-isopropylacrylamide for bioengineering applications. Prog. Polym. Sci., 2007, 32:534-595. DOI: 10.1016/j.progpolymsci.2007.01.006.

[9] Beija M., Marty J. D., Destarac M., RAFT/MADIX polymers for the preparation of polymer/inorganic nanohybrids. Prog. Polym. Sci., 2011, 36:845-886. DOI: 10.1016/j.progpolymsci.2011.01.002.

[10] Plummer R., Hill D. J. T., Whittaker A. K., Solution Properties of Star and Linear Poly(N-isopropylacrylamide). Macromolecules, 2006, 39:8379-8388. DOI: 10.1021/ma0614545.

[11] Nguyen H. H., Brulet A., Goudouneche D., Satin Aguet P., Lauth de Viguerie N., Marty J. D., The effect of polymer branching and average molar mass on the formation, stabilization and thermoresponsive properties of gold nanohybrids stabilized by poly(N-isopropylacrylamides). Polym. Chem., 2015, 6:5838-5850. DOI: 10.1039/c5py00659g.

[12] Nguyen H. H., Payré B., Fitremann J., Lauth de Viguerie N., Marty J. D., Thermoresponsive Properties of PNIPAM-Based Hydrogels: Effect of Molecular Architecture and Embedded Gold Nanoparticles. Langmuir, 2015, 31:4761-4768. DOI: 10.1021/acs.langmuir.5b00008.

[13] Sistach S., Beija M., Rahal V., Brûlet A., Marty J. D., Destarac M., Mingotaud C., Thermoresponsive Amphiphilic Diblock Copolymers Synthesized by MADIX/RAFT: Properties in Aqueous Solutions and Use for the Preparation and Stabilization of Gold Nanoparticles. Chem. Mater., 2010, 22:3712-3724. DOI: 10.1021/cm100674p.

[14] Xiao Z. P., Yang K. M., Liang H., Lu J., Synthesis of magnetic, reactive, and thermoresponsive Fe_3O_4 nanoparticles via surface-initiated RAFT copolymerization ofN-isopropylacrylamide and acrolein. J. Polym. Sci. A Polym. Chem., 2010, 48:542-550. DOI: 10.1002/pola.23752.

[15] Zhao X. G., Coutelier O., Nguyen H. H., Delmas C., Destarac M., Marty J. D., Effect of copolymer composition of RAFT/MADIX-derived N-vinylcaprolactam/N-vinylpyrrolidone statistical copolymers on their thermoresponsive behavior and hydrogel properties. Polym. Chem., 2015, 6:5233-5243. DOI: 10.1039/c5py00606f.

[16] Kermagoret A., Mathieu K., Thomassin J. M., Fustin C. A., Duchêne R., Jérôme C., Detrembleur C., Debuigne A., Double thermoresponsive di- and triblock copolymers based on N-vinylcaprolactam and N-vinylpyrrolidone: synthesis and comparative study of solution behaviour. Polym. Chem., 2014, 5:6534-6544. DOI: 10.1039/c4py00852a.

[17] Destarac M., Papon A., Van Gramberen E., Karagianni K., MADIX Thermoresponsive Amphiphilic Block Copolymers as Stimulable Emulsion Stabilizers. Aust. J. Chem., 2009, 62:1488-1491. DOI: 10.1071/CH09227.

[18] Baranowska-Korczyc A., Stelmach E., Paterczyk B., Maksymiuk K., Michalska A., Ultrasmall Self-Assembly poly(N-isopropylacrylamide-butyl Acrylate) (polyNIPAM-BA) Thermoresponsive Nanoparticles. J. Colloid Interface Sci., 2019, 542:317-324. DOI: 10.1016/j.jcis.2019.02.004

[19] Škvarla J., Zedník J., Šlouf M., Pispas S., Štěpánek M., Poly(N-isopropyl acrylamide)-block-poly(n-butyl acrylate) thermoresponsive amphiphilic copolymers: Synthesis, characterization and self-assembly behavior in aqueous solutions. Eur. Polym. J., 2014, 61:124-132. DOI: 10.1016/j.eurpolymj.2014.10.002.

[20] Blackman L. D., Wright D. B., Robin M. P., Gibson M. I., O'Relly R. K., Effect of Micellization on the Thermoresponsive Behavior of Polymeric Assemblies. ACS Macro Lett., 2015, 4:1210-1214. DOI: 10.1021/acsmacrolett.5b00551.

[21] Park J. H., Jang J. W., Sim J. H., Kim I. J., Lee D. J., Lee Y. H., Park S. H., Kim H. D., Preparation and Properties of Thermoresponsive P(N-Isopropylacrylamide-co-butylacrylate) Hydrogel Materials for Smart Windows. Int. J. Polym. Sci., 2019, 3824207. DOI: 10.1155/2019/3824207.

[22] Liu, X., Coutelier, O., Harrisson, S., Tassaing, T., Marty, J. D., Destarac, M., Enhanced Solubility of Polyvinyl Esters in $ScCO_2$ by Means of Vinyl Trifluorobutyrate Monomer. ACS Macro Lett., 2015, 4: 89-93. DOI: 10.1021/mz500731p.

[23] Destarac M., Papon A., Van Gramberen E., Karagianni K., MADIX Thermoresponsive Amphiphilic Block Copolymers as Stimulable Emulsion Stabilizers. Australian J. Chem., 2009, 62: 1488-1491. DOI: 10.1071/CH09227.

[24] Lindner P., Zemb T., Neutron, X-rayand light scattering: introductionto an investigative tool for colloidal and polymeric systems. North-Holland, Amsterdam. 1991, p19.

[25] Jacquin M., Muller P., Lizarraga G., Bauer C., Cottet H., Theodoly O., Characterization of Amphiphilic Diblock Copolymers Synthesized by MADIX Polymerization Process. Macromolecules, 2007, 40:2672-2682. DOI: 10.1021/ma062600+.

[26] Guinaudeau A. Towards sustainable development of RAF/MADIX polymerization: low temperature initiation and environment-friendly reaction media. Université de Toulouse. 2010.

[27] Mueller A. H. E., Zhuang R. G., Yan D. Y., Litvinenko G., Kinetic Analysis of "Living" Polymerization Processes Exhibiting Slow Equilibria. 1. Degenerative Transfer (Direct Activity Exchange between Active and "Dormant" Species). Application to Group Transfer Polymerization. Macromolecules, 1995, 28:4326-4333. DOI: 10.1021/ma00116a040.

[28] Wang X. H., Qiu X. P., Wu C., Comparison of the Coil-to-Globule and the Globule-to-Coil Transitions of a Single Poly(N-isopropylacrylamide) Homopolymer Chain in Water. Macromolecules, 1998, 31:2972-2976. DOI: 10.1021/ma971873p.

[29] Förster S., Zisenis M., Wenz E., Antonietti M., Micellization of strongly segregated block copolymers. J. Chem. Phys. 1996, 104:9956-9970. DOI: 10.1063/1.471723.

[30] Kujawa P., Aseyev V., TenhuH., WinnikF. M., Temperature-Sensitive Properties of Poly(N-isopropylacrylamide) Mesoglobules Formed in Dilute Aqueous Solutions Heated above Their Demixing Point. Macromolecules, 2006, 39:7686-7693. DOI: 10.1021/ma061604b.

[31] Ye J. Xu J., Hu J. M., Wang X. F., Zhang G. Z., Liu S. Y., WuC., Comparative Study of Temperature-Induced Association of Cyclic and Linear Poly(N-isopropylacrylamide) Chains in Dilute Solutions by Laser Light Scattering and Stopped-Flow Temperature Jump. Macromolecules, 2008, 41:4416-4422. DOI: 10.1021/ma702196g.

[32] Kujawa P., Tanaka F., Winnik F. M., Temperature-Dependent Properties of Telechelic Hydrophobically Modified Poly(N-isopropylacrylamides) in Water: Evidence from Light Scattering and

Fluorescence Spectroscopy for the Formation of Stable Mesoglobules at Elevated Temperatures. Macromolecules, 2006, 39:3048-3055. DOI: 10.1021/ma0600254.

[33] Durme K. V., Verbrugghe S., Du Prez F. E., Van MeleB., Influence of Poly(ethylene oxide) Grafts on Kinetics of LCST Behavior in Aqueous Poly(N-vinylcaprolactam) Solutions and Networks Studied by Modulated Temperature DSC. Macromolecules, 2004, 37:1054-1061. DOI: 10.1021/ma035319t.

[34] Li B., Thompson M. E., Phase transition in amphiphilic poly(N-isopropylacrylamide): controlled gelation. Phys. Chem. Chem. Phys., 2018, 20:13623-13631. DOI: 10.1039/c8cp01609g.

[35] Füllbrandt M., von Klitzing R., Schönhals A., Probing the phase transition of aqueous solutions of linear low molecular weight poly(N-isopropylacrylamide) by dielectric spectroscopy. Soft. Matter., 2012, 8:12116–12123. DOI: 10.1039/c2sm26826d.

[36] Jakubowski W., Juhari A., Best A., Koynov K., Pakula T., Matyjaszewski K., Comparison of thermomechanical properties of statistical, gradient and block copolymers of isobornyl acrylate and n-butyl acrylate with various acrylate homopolymers. Polymer. 2008, 49:1567-1578. DOI: 10.1016/j.polymer.2008.01.047.

[37] Fijten M. W. M., Kranenburg J. M., Thijs H. M. L., Paulus R. M., van Lankvelt B. M., de Hullu J., Springintveld M., Thielen D. J. G., Tweedie C. A., Hoogenboom R., Van Vliet K. J., Schubert U. S., Synthesis and Structure-Property Relationships of Random and BlockCopolymers: A Direct Comparison for Copoly(2-oxazoline)s. Macromolecules, 2007, 40:5879-5886. DOI: 10.1021/ma070720r.

[38] Hou L., Wu P. Y., Comparison of LCST-transitions of homopolymer mixture, diblock and statistical copolymers of NIPAM and VCL in water. Soft Matter., 2015, 11:2771-278, DOI: 10.1039/C5SM00026B.

[39] Dionzou M., Morère A., Roux C., Lonetti B., Marty, J. D., Mingotaud, C., Joseph P., Goudounèche D., Payré B., Léonetti M., Mingotaud A. F., Comparison of methods for the fabrication and the characterization of polymer self-assemblies: what are the important parameters? Soft Matter., 2016, 12: 2166-2176. DOI: 10.1039/C5SM01863C.

[40] Nicolai T., Colombani O., Chassenieux C., Dynamic polymeric micelles versus frozen nanoparticles formed by block copolymers. Soft Matter., 2010, 6:3111-3118. DOI: 10.1039/B925666K.

[41] Jacquin M., Muller P., Talingting-Pabalan R., Cottet H., Berret J. F., Futterer T., Théodoly O., Chemical Analysis and Aqueous Solution Properties of Charged Amphiphilic Block Copolymers PBA-b-PAA Synthesized by MADIX. J. Coll. Interf. Sci. 2007, 316:897-911. DOI: 10.1016/j.jcis.2007.08.025.

[42] Colombani O., Ruppel M., Burkhardt M., Drechsler M., Schumacher M., Gradzielski M., Schweins R., Müller A. H. E., Structure of Micelles of Poly(n-butyl acrylate)-block-poly(acrylic acid) Diblock Copolymers in Aqueous Solution. Macromolecules, 2007, 40:4351-4362. DOI: 10.1021/ma0609580.

[43] Garnier S., Laschewsky A., Synthesis of New Amphiphilic Diblock Copolymers and Their Self-Assembly in Aqueous Solution. Langmuir, 2006, *22*:4044-4053. DOI: 10.1021/ma0506785.

[44] Lejeune E., Drechsler M., Jestin J., Müller A. H. E., Chassenieux C., Colombani O., Amphiphilic Diblock Copolymers with a Moderately Hydrophobic Block: Toward Dynamic Micelles. Macromolecules, 2010, 43:2667-2671. DOI: 10.1021/ma902822g.

[45] Liu X., Wang M., Harrisson S., Debuigne A., Marty J. D., Destarac M., Enhanced Stabilization of Water-scCO_2 Interface by Block-like Spontaneous Gradient Copolymers, ACS Sus. Chem. Eng., 2017, 5:9645-9650. DOI: 10.1021/acssuschemeng.7b02779.

Figure captions:

Scheme 1. Synthesis of PNIPAM-b-PBA-b-PNIPAM copolymers by RAFT/MADIX polymerization.

Figure 1. Size exclusion chromatograms (RI response) in THF of $PNIPAM_{2.5k}$-*b*-PBA_{5k}-*b*-$PNIPAM_{2.5k}$ (red line) and PBA_{5k} (blue line).

Figure 2. Turbidimetry (A and B), DLS (C) and DSC (D) measurements of a 0.1 wt.% (or 1 wt.% for DSC) aqueous solutions of $PNIPAM_{4k}$-*b*-PBA_{2k}-*b*-$PNIPAM_{4k}$ triblock copolymer. A) Transmittance monitored at 500 nm on heating and cooling (1 °C·min^{-1}). B) Extrapolation of measured inflexion points determine from turbidimetry curves at different heating/cooling rates. C) Hydrodynamic diameter obtained from DLS measurements on heating. D) DSC thermograms recorded on heating and cooling at the rate of 1 °C·min^{-1}.

Figure 3. Cloud point temperatures T_c (peak maximum) obtained by DSC on heating (red plain marks) or cooling (blue open marks) for PNIPAM homopolymer and statistical, diblock and triblock PNIPAM-based copolymers at a concentration of 1 wt.%.

Figure 4. (A) Scattering intensity in absolute units (cm^{-1}) of D_2O solutions of (0.1 wt.%) $PNIPAM_{4k}$-*b*-PBA_{2k}-*b*-$PNIPAM_{4k}$ (+) and $PNIPAM_{2.5k}$-*b*-PBA_{5k}-*b*-$PNIPAM_{2.5k}$ (o) measured at 20 °C. Lines are the best fits to a model of polydisperse sphere with a log-normal distribution. (B) Representative TEM micrograph of aggregates formed by $PNIPAM_{4k}$-*b*-PBA_{2k}-*b*-$PNIPAM_{4k}$ at 20 °C stained with uranyl acetate (TEM deposit performed above T_c).

Figure 5. (A) Scattering intensity in absolute units (cm^{-1}) of D_2O solutions of (0.1 wt.%) $PNIPAM_{4k}$-*b*-PBA_{2k}-*b*-$PNIPAM_{4k}$ (+) and $PNIPAM_{2.5k}$-*b*-PBA_{5k}-*b*-$PNIPAM_{2.5k}$ (o) measured at 36 °C. Lines are the best fits to a model of polydisperse sphere with Gaussian distribution. (B) TEM image (negative staining) of aggregates formed above the cloud point for $PNIPAM_{4k}$-*b*-PBA_{2k}-*b*-$PNIPAM_{4k}$ (TEM deposit performed above T_c).

Figure 6. Photographs of the observed phase transition for $PNIPAM_{4k}$-*b*-PBA_{2k}-*b*-$PNIPAM_{4k}$ triblock structure at a concentration of 20 wt.% as function of temperature: Transparent Solution (TS phase)→ opaque solution (OS) → opaque gel phase (OG) → dehydrated gel phase (DG). Phase diagram of aqueous polymer solutions for $PNIPAM_{4k}$-*b*-PBA_{2k}-*b*-$PNIPAM_{4k}$ (left) and PBA_{2k}-*b*-$PNIPAM_{8k}$ (right) as a function of temperature and concentration.

Figure 7. Temperature – dependent storage G' (empty marks) and loss G'' (filled marks) moduli for $PNIPAM_{4k}$-*b*-PBA_{2k}-*b*-$PNIPAM_{4k}$ and PBA_{2k}-*b*-$PNIPAM_{8k}$ (20 wt.% aqueous solutions) with heating rate at 1 °C·min^{-1}.

Figure 8. Images obtained from cryo-SEM of gel structures at 40 °C obtained from $PNIPAM_{4k}$-*b*-PBA_{2k}-*b*-$PNIPAM_{4k}$ (noted 4-2-4), PBA_{2k}-*b*-$PNIPAM_{8k}$ (noted 2-*b*-8), $PNIPAM_{2.5k}$-*b*-PBA_{5k}-*b*-$PNIPAM_{2.5k}$ (noted 2.5-5-2.5) and PBA_{5k}-*b*-$PNIPAM_{5k}$ (noted 5-*b*-5) (size distribution of pores are given as insets).

Scheme 2. Schematic behaviour of the different polymer in solution as a function of concentration and temperature.

Table 1. Characteristics of various copolymers prepared by RAFT/MADIX polymerization: $\bar{M}_n$, dispersities (Đ) and glass transition temperatures (T_g).

PBA /PNIPAM	Sample	$\bar{M}_n$ (g·mol^{-1})[a]	$Đ$ [a]	T_g [b] (°C)	ΔC_p [b] (J·g^{-1}.K^{-1})
0.5k/9.5k	P(BA-*s*-PNIPAM)$_{10k}$ (0.05:0.95 w)	10620	1.30	111.90	0.74
1k/9k	P(BA-*s*-PNIPAM)$_{10k}$ (0.1:0.9 w)	11230	1.57	114.20	0.71
2k/8k	PBA$_{2k}$-*b*-PNIPAM$_{8k}$	10000	1.16	108.90	0.20
	P(BA-*s*-PNIPAM)$_{10k}$ (0.2:0.8 w)	9100	1.81	100.40	0.63
	PNIPAM$_{4k}$-*b*-PBA$_{2k}$-*b*-PNIPAM$_{4k}$	8960	1.40	100.60	0.28
5k/5k	PBA$_{5k}$-*b*-PNIPAM$_{5k}$	9400	1.25	-48.00 106.70	0.10 0.20
	PNIPAM$_{2.5k}$-*b*-PBA$_{5k}$-*b*-PNIPAM$_{2.5k}$	11000	1.23	-35.20 86.21	0.10 0.28
8k/2k	PBA$_{8k}$-*b*-PNIPAM$_{2k}$	10100	1.20	-44.00 133.00	0.40 0.10
	PNIPAM$_{1k}$ -b-PBA$_{8k}$-*b*-PNIPAM$_{1k}$	9900	1.36	-41.70	0.56
PBA	PBA$_{2k}$	2400	1.38	-50.70	0.50
	PBA$_{5k}$	5750	1.35	-50.60	0.50
	PBA$_{8k}$	9500	1.30	-50.70	0.50
PNIPAM	PNIPAM$_{8k}$	17600	1.27	127.90	0.40
	PNIPAM$_{10k}$	21300	1.31	126.20	0.46

[a] SEC was performed in THF with RI-MALS detection expect in the case o f PNIPAM homopolymers for which SEC was performed in DMF/LiBr (10 mmol·L^{-1}) with PMMA calibration (40 °C, flow rate: 1mL·min^{-1}). In the latter case the chosen conditions led to an overestimate the given mass by a factor of two. [b] Glass transitions measured at a heating rate of 10°C·min^{-1}.

Table 2. Cloud points (T_c) and DLS, TEM and SANS results on polymer aqueous solutions at 20 ºC and 40 ºC

Polymer	Cloud point	Radius (nm) at 20 °C			Radius (nm) at 40 °C		
	Tc[a]	$\langle R\rangle_{TEM}$	$\langle R_h\rangle_{DLS}$	$\langle R\rangle_{SANS}$	$\langle R\rangle_{TEM}$	$\langle R_h\rangle_{DLS}$	$\langle R\rangle_{SANS}$
$PNIPAM_{10k}$	32.3	-	3±2	-	-	243±97	-
PBA_{2k}-*b*-$PNIPAM_{8k}$	27.6	11.0±1.5	14±3	8±1	-	57±3	52±7
$PNIPAM_{4k}$-*b*-PBA_{2k}-*b*-$PNIPAM_{4k}$	25.1	10.6±2.3	10.5±2.0	4.9±2.0**	21.6±3.5	78±2	39±11
PBA_{5k}-*b*-$PNIPAM_{5k}$	26.4	20.5±5.0	31±6	20.5±3.5	-	66±1	53±8
$PNIPAM_{2.5k}$-*b*-PBA_{5k}-*b*-$PNIPAM_{2.5k}$	21.7		53.5±2.5	9±5**		123±2	46±7

[a] Obtained from DSC measurements (1 wt.% in cooling mode). Radius values are given for 0.1 wt.% polymer solutions. Preparation methods (direct solubilization, liposomes-like, …) do not influence Rh. Note: Errors in DLS results were calculated by multiplying polydispersity index values by the mean hydrodynamic radius values. Error in the fits results from SANS were calculated by multiplying the distribution by the radius values. ** log-normal distribution